DOI:
10.1016/j.jaac.2015.05.011

Document Version
Peer reviewed version

Citation for published version (APA):
Bos, D. J., Merchán-Naranjo, J., Martínez, K., Pina-Camacho, L., Balsa, I., Boada, L., ... Janssen, J. (2015). Reduced Gyrification Is Related to Reduced Interhemispheric Connectivity in Autism Spectrum Disorders. Journal of the American Academy of Child and Adolescent Psychiatry, 54(8), 668-676. [1225]. 10.1016/j.jaac.2015.05.011

Accepted Manuscript

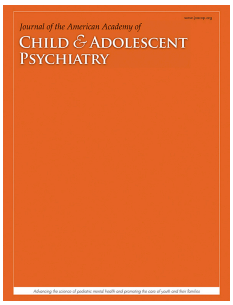

Reduced Gyrification is Related to Reduced Interhemispheric Connectivity in Autism Spectrum Disorders

Dienke J. Bos, MSc, Jessica Merchán-Naranjo, MSc, Kenia Martínez, PhD, Laura Pina-Camacho, MD, Ivan Balsa, BSc, Leticia Boada, MSc, Hugo Schnack, PhD, Bob Oranje, PhD, Manuel Desco, MD, PhD, Celso Arango, MD, PhD, Mara Parellada, MD, PhD, Sarah Durston, PhD, Joost Janssen, PhD

PII: S0890-8567(15)00350-0

DOI: 10.1016/j.jaac.2015.05.011

Reference: JAAC 1225

To appear in: *Journal of the American Academy of Child & Adolescent Psychiatry*

Received Date: 5 December 2014

Revised Date: 22 May 2015

Accepted Date: 27 May 2015

Please cite this article as: Bos DJ, Merchán-Naranjo J, Martínez K, Pina-Camacho L, Balsa I, Boada L, Schnack H, Oranje B, Desco M, Arango C, Parellada M, Durston S, Janssen J, Reduced Gyrification is Related to Reduced Interhemispheric Connectivity in Autism Spectrum Disorders, *Journal of the American Academy of Child & Adolescent Psychiatry* (2015), doi: 10.1016/j.jaac.2015.05.011.

Reduced Gyrification is Related to Reduced Interhemispheric Connectivity in Autism Spectrum Disorders

RH = Gyrification and Connectivity in Autism

Dienke J. Bos, MSc; Jessica Merchán-Naranjo, MSc; Kenia Martínez, PhD; Laura Pina-Camacho, MD; Ivan Balsa, BSc; Leticia Boada, MSc; Hugo Schnack, PhD; Bob Oranje, PhD; Manuel Desco, MD, PhD; Celso Arango, MD, PhD; Mara Parellada, MD, PhD; Sarah Durston, PhD; Joost Janssen, PhD

Supplemental material cited in this article is available online.

Accepted May 29, 2015

Ms. Bos and Drs. Oranje, Schnack, Durston, and Janssen are with Brain Center Rudolf Magnus, University Medical Center Utrecht, The Netherlands. Ms. Merchán-Naranjo, Ms. Boada, and Drs. Martinez, Arango, Parellada, and Janssen are with Hospital General Universitario Gregorio Marañón, School of Medicine, Universidad Complutense, Madrid, Spain. Ms. Merchán-Naranjo, Ms. Boada, and Drs. Martinez, Arango, Parellada, and Janssen are also with the Instituto de Investigación Sanitaria Gregorio Marañón (IISGM), Madrid. Mr. Balsa and Dr. Desco are also with IISGM. Ms. Merchán-Naranjo and Ms. Boada and Drs. Pina-Camacho, Desco, Arango, Parellada, and Janssen are also with the Ciber del área de Salud Mental (CIBERSAM), Madrid. Dr. Pina-Camacho is also with the Institute of Psychiatry, King's College London, UK. Dr. Desco is also with Universidad Carlos III de Madrid.

This study is supported by the Spanish Ministry of Economy and Competitiveness, Instituto de Salud Carlos III, CIBERSAM, the Ramon y Cajal Program, the CDTI under the CENIT Program (AMIT Project), Madrid Regional Government (S2010/BMD-2422 AGES), European Union Structural Funds and European Union Seventh Framework Programme under grant agreements FP7-HEALTH-2009-2.2.1-2-241909 (Project EU-GEI), FP7-HEALTH-2009-2.2.1-3-242114 (Project OPTiMISE), FP7- HEALTH-2013-2.2.1-2- 603196 (Project PSYSCAN), and FP7- HEALTH-2013-2.2.1-2-602478 (Project METSY); the ERA-NET NEURON (Network of European Funding for Neuroscience Research) (PIM2010ERN-00642), Fundación Alicia Koplowitz (FAK2012, FAK2013), Fundación Mutua Madrileña (FMM2009), and Caja Navarra. Support for ABIDE-NYU Langone coordination and data aggregation was partially provided by National Institute of Mental Health (K23MH087770, R03MH09632, and BRAINSRO1MH094639-01), National Institutes of Health (R21MH084126), Autism Speaks, and the Leon Levy Foundation; and gifts from Joseph P. Healey and the Stavros Niarchos Foundation.

The authors thank all children, adolescents, and their parents for participating in this study and Yasser Alemán-Gómez, PhD, of the Instituto de Investigación Sanitaria Gregorio Marañón, for technical support. The authors also thank all the members of the ABIDE, Michael P. Milham, PhD, of the New York University Medical Center, and INDI team (http://fcon_1000.projects.nitrc.org/) for supporting the ABIDE effort.

Disclosure: Drs. Martínez, Pina-Camacho, Schnack, Oranje, Desco, Arango, Parellada, Durston, Janssen, and Ms. Bos, Ms. Merchán-Naranjo, Mr. Balsa, and Ms. Boada report no biomedical financial interests or potential conflicts of interest.

Correspondence to Dienke J. Bos, NICHE Lab, Department of Psychiatry, Brain Center Rudolf Magnus, University Medical Center Utrecht, HP A.01.126, Heidelberglaan 100, 3584 CX Utrecht, The Netherlands; email: d.j.bos-2@umcutrecht.nl

Abstract

Objective. Autism spectrum disorders (ASD) have been associated with atypical cortical grey and subcortical white matter development. Neurodevelopmental theories postulate that a relation between cortical maturation and structural brain connectivity may exist. We therefore investigated the development of gyrification and white matter connectivity and their relationship in individuals with ASD and their typically developing peers.

Method. T1- and diffusion-weighted images were acquired from a representative sample of 30 children and adolescents with ASD (aged 8 to 18 years), and 29 typically developing children matched for age, sex, hand preference, and socioeconomic status. The FreeSurfer suite was used to calculate cortical volume, surface area, and gyrification index. Measures of structural connectivity were estimated using probabilistic tractography and tract-based spatial statistics (TBSS).

Results. Left prefrontal and parietal cortex showed a relative, age-dependent decrease in gyrification index in children and adolescents with ASD compared to typically developing controls. This result was replicated in an age and IQ-matched sample provided by the Autism Brain Imaging Data Exchange (ABIDE) initiative. Furthermore, tractography and TBSS showed a complementary pattern, where left prefrontal gyrification was negatively related to radial diffusivity in the forceps minor in participants with ASD.

Conclusion. The present study builds on earlier findings of abnormal gyrification and structural connectivity in the prefrontal cortex in ASD. It provides a more comprehensive neurodevelopmental characterization of ASD, involving interdependent changes in microstructural white and cortical grey matter. The findings of related abnormal patterns of gyrification and white matter connectivity support the notion of the intertwined development of two major morphometric domains in ASD.

Keywords: Autism spectrum disorders, gyrification index, structural connectivity, development, forceps minor

Introduction

Autism spectrum disorders (ASD) are pervasive developmental disorders characterized by persistent deficits in social communication and social interaction and the presence of restricted, repetitive patterns of behavior, interests, or activities [1]. The early onset of symptoms, typically well before the age of three, has been suggested to coincide with an overgrowth of cortical volume during the first years of life followed by a gradual decrease [2,3]. This pattern appears not to be limited to specific brain areas, but to involve the entire cortex [4,5]. Post mortem research of childhood ASD has shown an excess of neurons and disorganization in all cortical laminae of the prefrontal cortex (PFC), suggesting that increases in brain size have an early onset, possibly during prenatal neurodevelopment [6,7].

The brain's folding pattern is a strong marker of prenatal neurodevelopment [8]. Gyrification commences in gestational week 16 and greatly intensifies during the third trimester when the brain folds in on itself, as cortical volume—mostly white matter (WM)—and surface area (SA) rapidly increase [9]. To date, multiple theories have tried to explain the pattern of cortical folding. Tension-induced folding suggests that strongly interconnected regions pull towards each other and lead to the formation of gyri, whereas more sparsely connected fibers elongate to leave room for sulci [10]. The "grey matter hypothesis" suggests that gyrification may be the result of cell proliferation in the outer subventricular zone during early gestation [11]. This hypothesis is based on findings in transgenic mice, which showed increased cerebral cortical SA and human-like folds after controlling the cell cycle exit of neural precursors in the outer subventricular zone [12].

Whole-brain studies have indeed shown a pattern of increased sulcal complexity [13] and differences in cortical shape [14] and sulcal pattern [15,16] in children and adolescents with ASD. However, two recent studies using 3D methodologies in ASD have reported conflicting results, with the first reporting increased gyrification in adolescents with ASD [17] and the second reporting decreased gyrification in a slightly younger sample [18].

Gyrification and white matter development seem inextricably tied [19], continuously remodeling the cortex throughout development [20]. Schaer et al.[18] interestingly showed a relationship between reduced gyrification index (GI) and reduced white matter connectivity in a small group of low-functioning children with ASD, where right prefrontal gyrification was positively correlated with the number of white matter fibers in ASD. This ties in with an ever-growing body of literature reporting development changes in (interhemispheric) connectivity in ASD, especially in prefrontal tracts such as the forceps minor (reviewed in [21,22]).

However, considerable heterogeneity in symptom presentation and severity and the wide range of analysis methods used in these studies may have contributed to mixed reports on the relationship between gyrification and connectivity to date. In the current study, we set out to investigate the relationship between gyrification and white matter connectivity with a focus on age-related changes in a sample of children and adolescents with ASD. We specifically aimed at investigating the PFC given previous literature. We hypothesized that GI would be reduced in children and adolescents with ASD. Furthermore, we used an independent sample of high-functioning children and adolescents with ASD from the Autism Brain Imaging Data Exchange (ABIDE) initiative to replicate our findings [23]. We further hypothesized that this reduced cortical gyrification would be related to reduced connectivity, in line with earlier findings in a sample of lower functioning children with ASD and current neurodevelopmental theories.

Method

Participants

Thirty children and adolescents aged 8 to 18 years with ASD, as well as 29 typically developing controls, were recruited, matched for age, sex, hand preference, and socio-economic status (Table 1). Children and adolescents with ASD were recruited through family associations and the outpatient clinic of the Child and Adolescent Psychiatry Department at Hospital General Universitario Gregorio Marañon in Madrid, Spain (hereafter referred to as the Madrid sample) [24]. Typically developing controls were recruited from the community at publicly funded schools with characteristics similar to those attended by participants with ASD and in the same geographic area [25].

Children and adolescents with ASD were included if they fulfilled *DSM-IV-TR* criteria for pervasive developmental disorders at the time of assessment [26] and the Gillberg criteria [27] for Asperger syndrome. Board-certified child and adolescent psychiatrists with extensive experience in the field of ASD conducted all diagnostic assessments. Detailed information on the diagnostic assessments is given in Supplement 1 (available online).

Exclusion criteria for all participants included intellectual disabilities per *DSM-IV* criteria [26], any neurological disorder, history of head trauma with loss of consciousness, and other contraindications to magnetic resonance imaging (MRI) scanning. The institutional review board of the Hospital General Universitario Gregorio Marañon in Madrid approved the protocol and informed consent form. All parents or legal guardians gave written informed consent after receiving complete information about the study, and all participants provided assent.

Demographic, Clinical and Cognitive Assessment

For all participants, demographic data, including age, sex, ethnicity, parent and participant years of education, and socioeconomic status (SES)—assessed with the Hollingshead-Redlich

scale[28]—were recorded at inclusion (Table 1). Psychosocial functioning was assessed for all participants using the Children's Global Assessment Scale (CGAS) [29,30]. For the typically developing controls, an estimated IQ was calculated using the vocabulary and block-design tests of the Wechsler Intelligence Scale for Children (WISC-R[31]) for participants less than 16 years of age, or the Wechsler Adult Intelligence Scale (WAIS-III: [32]) for participants aged 16 years or older. For the group with ASD, full-scale IQ was obtained using the WISC-R or WAIS-III depending on the age of the participant [33]. As lower IQ may be considered typical of the ASD phenotype, IQ was not entered as a covariate in any of the designs to prevent partialling out variance that is potentially relevant to the disorder [34]. Hand preference was assessed using item five of the Neurological Evaluation Scale (NES) [35], which evaluates hand preference during several activities such as writing, throwing a ball, or opening a jar.

MRI Acquisition and Image Analyses

All participants were scanned on a single Philips Intera 1.5T MRI scanner (Philips Medical Systems, The Netherlands). MRI acquisition parameters are described in Supplement 1 (available online).

Lobar SA and GI

The FreeSurfer analysis suite (v5.3) was used to generate white and pial surfaces and an automated cortical lobar parcellation (prefrontal, parietal, temporal, and occipital) [36–38], not including the cingulate cortex, as this structure cannot be assigned to a single lobe. SA was calculated per lobe from the pial surface. Automated segmentation results were reviewed for quality and corrected by trained experts as necessary. GI was calculated per lobe, separately for the left and right hemispheres following the method by Su et al. [39] and is further explained in Supplement 1 and Figure S1 (available online). This method uses the standard definition for GI as formulated by Zilles et al [40]:

$$Gyrification\ Index_{Lobe\,i} = \frac{Pial\ Surface\ Area_{Lobe\,i}}{Hull\ Surface\ Area_{Lobe\,i}} \quad (1.0)$$

Replication Sample

The methods described earlier for measuring cortical volume, SA, and GI, in the Madrid sample were repeated in a similar, independent sample provided by the ABIDE initiative (Table 2) [23]. A full description of data acquisition and inclusion of participants in this replication sample is given in Supplement 1 and Tables S2-4 (available online).

Forceps Minor Tractography

The forceps minor was chosen as region of interest based on previous literature showing reductions in anterior corpus callosum area in ASD [41,42]. A detailed description of the diffusion tensor imaging (DTI) preprocessing and quality control can be found in Supplement 1 and Table S5 (available online). Anatomically constrained probabilistic diffusion tractography was carried out using the Tracts Constrained by UnderLying Anatomy (TRACULA) tool within FreeSurfer [43] using default settings. Mean values of fractional anisotropy (FA), axial diffusivity (AD), and radial diffusivity (RD) of the forceps minor tract were provided by TRACULA (thresholding the pathway distribution at 20% of its maximum value for all participants). AD and RD values were multiplied by 100. Analyses run with FA, AD, and RD averaged from just the center of the forceps minor tract did not change the results in any meaningful way.

Tract-Based Spatial Statistics

Voxelwise statistical analyses of FA and RD data were carried out using Tract-Based Spatial Statistics (TBSS) [44] in FMRIB Software Library (FSL) [45]. TBSS projects FA, AD, and RD

from all participants onto a mean tract skeleton before applying voxelwise cross-subject statistics. Individual measurements averaged over the largest clusters that showed a significant effect were extracted and plotted.

Statistics

Normality of the distribution and equality of variance between groups (homoscedasticity) was confirmed before all analyses. Between-group differences in demographic, clinical, cognitive, and whole-brain and lobe features (cortical volume, SA and GI) were assessed using Student's t-tests for independent samples for continuous variables and Chi-square tests for categorical variables.

For each lobe and the forceps minor, we used analysis of covariance (ANCOVA) to examine whether age differentially explained variance in SA, GI (for lobes), and mean FA, AD, and RD (for forceps minor) between groups. In each model, diagnosis was set as independent variable and age as covariate. Note that a significant main effect of diagnosis was not further explored if it was accompanied by a significant diagnosis x age interaction. Medication status did not show any significant effects and was thus not used as a covariate in the final analyses.

TBSS voxelwise analyses for FA, AD, and RD were carried out across participants for each point of the common skeleton. We applied the same ANCOVA model as described above at each voxel of the skeleton. A permutation-based approach was performed to control for the family-wise error (FWE; [46]), using threshold-free cluster enhancement (TFCE) and a number of permutations set at 5000 in FSL's Randomise (FMRIB Software Library Randomise v2.9).

The relationship between GI and connectivity was assessed using ANCOVA on the standardized residuals (corrected for age) of GI and the connectivity measures. Effect sizes are given as Cohen's d.

Results

GI and SA

There was an interactive effect of diagnosis x age on left prefrontal and parietal GI, where participants with ASD show a relative decrease with age as compared to typically developing controls (Figure 1 and Figures S2-S5, available online). These results remained significant when two female participants were removed from the analyses. There was no main effect of diagnosis in the absence of a diagnosis x age interaction. Finally, there were no effects of whole-brain GI and SA (Table S1, available online) and SA per lobe (Figures S2-S5, available online).

GI and SA: Replication in an Age and IQ-Matched Independent Sample

As Figure 1 shows, the significant diagnosis x age interactions for the left prefrontal and parietal cortex GI were replicated in the ABIDE set. For SA there was no significant diagnosis x age interaction (left prefrontal: F=0.75, p=.39, d=0.17, left parietal: F=2.89, p=.09, d=0.34), nor a main effect of diagnosis alone (left prefrontal: F=0.43, p=.52, d=0.13, left parietal: F=2.28, p=.13, d=0.30).

Furthermore, as the replication sample was not fully matched on verbal IQ (VIQ: Table 2), the analyses were repeated in a slightly smaller but VIQ-matched subsample of 39 children with ASD and 56 typically developing children (Table S6, available online). In this subsample, the effect of the diagnosis x age interaction held for left prefrontal (F=3.83, p=.05, d=0.41), and parietal (F=4.59, p=.04, d=0.45) GI remained significant.

As the participants from the replication sample included more females than the Madrid sample (Table 2), we assessed whether the interaction was still significant after controlling for sex and found left prefrontal GI is significant at the trend level (F=3.66, p=.059), and the left parietal GI remains significant (F=5.47, p=.02).

Forceps Minor Tractography and TBSS

There was an effect of age (F=8.68, p<.01, d=0.79) and diagnosis x age (F=5.46, p=.02, d=0.63) on FA in the forceps minor in the Madrid sample. In addition, there were effects of age (F=6.40, p=.01, d=0.68), diagnosis (F=7.58, p=.01, d=0.74), and diagnosis x age (F=10.12, p<.01, d=0.86) on RD (Figure 2). There were no effects for AD. These findings were confirmed in the TBSS analyses (Figure 2), where we found a diagnosis x age interaction on FA and RD, but not on AD, within the same region (Montreal Neurological Institute [MNI] coordinates [mm] of the largest significant clusters: FA: x = 18, y = 17, z = 30; 2,581 voxels; RD: x = -18, y = 16, z = 29; 2,653 voxels). Figure 2 shows that these clusters overlap with the forceps minor.

The Relationship Between Forceps Minor Diffusion and Left Prefrontal Gyrification

To assess the age-independent relation between prefrontal GI and forceps minor FA and RD in the Madrid sample, we first linearly regressed out the effect of age on the left prefrontal GI, forceps minor FA and RD, and tested for a diagnosis x FA/RD interaction on the left prefrontal GI. A significant diagnosis x RD interaction (F=6.15, p=.02, d=0.67) but no significant diagnosis x FA interaction (F=2.89, p=.1, d=0.46) (Figure 3) was found. Pearson's correlations indeed showed RD and GI were significantly correlated in the group with ASD (r = -.50, p = .01), but not in the typically developing children (r = -.04, p = .84).

Discussion

The current study shows age-related differences in gyrification in the left prefrontal and parietal cortex in a representative sample of children and adolescents with ASD, while there were no differences in cortical SA within the age range studied. These results were replicated in a larger age- and IQ-matched independent sample including high-functioning individuals with ASD from the ABIDE initiative [23]. Furthermore, age-related differences were observed in anterior callosal forceps minor connectivity. These results suggest abnormalities in two major morphometric domains, which in addition seem negatively related in ASD.

The reported age-related differences in left prefrontal and parietal gyrification in ASD may reflect abnormal cortical maturation during childhood and adolescence. It has been suggested that in typically developing individuals, gyrification peaks during or even before toddlerhood [47,48] followed by a decrease in adolescence and adulthood [49,50]. Our results show that compared to typically developing children, this relative developmental decrease in gyrification may be more pronounced in individuals with ASD, and that it may follow a similar pattern as the possible progressive decrease in total brain volume that has been suggested in ASD [4].

The age-related decrease of gyrification in children and adolescents with ASD converges with earlier findings in studies with similar age ranges [17,18,51]. This suggests that differences in methodologies or group characteristics may indeed have contributed to inconsistencies with previous studies. However, the abnormal pattern of left prefrontal and parietal gyrification was observed both in low- and higher-functioning children and adolescents with ASD, indicating that on the regional level, gyrification is likely to be affected across different levels of IQ in individuals with ASD.

Interestingly, there was no interaction between group and age for cortical SA. Given the strong relationship between SA and cortical volume [52], this may imply that within this age range,

cortical morphological complexity rather than brain size is more defining in the pathophysiology of ASD. This notion fits with recently reported differences in cortical shape complexity in ASD without differences in cortical SA [17,53].

The forceps minor connects the medial and lateral parts of the PFC. In contrast with inconsistent findings of reduced gyrification in ASD, reduced interhemispheric connectivity—and specifically decreased forceps minor connectivity—has been reported consistently (for reviews see [21,22]). While FA typically increases throughout development, [54,55] mostly peaking well into adulthood,[56] the present study shows, in line with previous studies, that forceps minor development may not show these age-related gains in child and adolescent participants with ASD [57–59]. On the behavioral level, reduced forceps minor connectivity has indeed been related to restricted and stereotyped behavior [18,42]. The relevance of disruptions to the frontal-callosal forceps minor in ASD is further supported by findings from individuals with callosal agenesis (CA), a birth defect characterized by the complete or partial absence of corpus callosum. Individuals with CA experience autism-like symptoms such as impairments in social interaction and communication [60].

Finally, left prefrontal gyrification and forceps minor connectivity showed a negative, age-independent relation, suggesting a stable relationship between prefrontal gyrification and forceps minor radial diffusivity across childhood and adolescence in ASD. This relationship may reflect atypical neurodevelopmental processes that arise before childhood. Speculatively, at a young age, left prefrontal and parietal gyrification may even be increased in ASD. Such a relation could be hypothesized to be tied to the heightened presence of short-range intracortical white matter connections [10,53]: Increased left prefrontal and parietal gyrification during early brain development may then reflect local overgrowth of short-range connectivity at the expense of decreased long-range (forceps minor) connectivity [18,53,61]. This converges with the present understanding of ASD as a “disconnection syndrome,”[62] where connections, especially within or between the prefrontal cortices, are compromised [21]. When comparing the results from

tractography and TBSS, the group difference in FA appears to be driven primarily by a difference in RD. A change in RD, independent of axial diffusion, could indeed suggest myelination loss, or loss of axons in the forceps minor [63].

Strengths of this study lie in the multimodal approach allowing for the microstructural and macrostructural neuroanatomical characterization of the disorder, and in the replication of the gyrification results in a larger, independent, yet similar sample of individuals. There are, however, also limitations that need to be taken into consideration. In the Madrid sample, no measure of full-scale IQ was available for typically developing participants. Previous studies have shown that in typically developing individuals, the two subtests we used provide a reliable estimate of IQ [33]. Furthermore, even though IQ was not matched in the Madrid sample, parental education and SES (often used as an estimate of premorbid IQ in studies of other psychiatric disorders) did not differ significantly between the two groups. The similarity of the results in the IQ-matched replication sample further supports that differences in GI are likely present across a broad spectrum of ASD phenotypes. Further, due to the assessment of lobar GI, stretching over large patches of cortex, the regional correspondence with forceps minor connectivity may not be optimal. Even though the forceps minor branches out within the prefrontal cortex, more accurate spatial correspondence could potentially be achieved with local, vertex-wise GI metrics. However, such an approach would be more prone to partial volumning effects, which are minimized in the current study. Another limitation is the cross-sectional design of the study. Developmental studies will inarguably benefit from a longitudinal set-up to better deal with individual differences that are not adequately captured in cross-sectional designs. However, the results presented in the current study may provide a valuable framework for such future studies.

In conclusion we found evidence for decreased gyrification in children and adolescents with ASD, which was related to developmental changes in forceps minor connectivity. These findings provide a more comprehensive neuroanatomical characterization of ASD involving related microstructural white matter and macrostructural cortical grey matter changes. Our

findings of related abnormal patterns of gyrification and white matter connectivity support the notion of the intertwined development of two major morphometric domains in individuals with ASD.

References

1. American Psychiatric Association. *The Diagnostic and Statistical Manual of Mental Disorders: DSM 5*. Washington DC: American Psychiatric Publishing; 2013.
2. Courchesne E, Karns CM, Davis HR, et al. Unusual brain growth patterns in early life in patients with autistic disorder: an MRI study. *Neurology*. 2001;57(2):245–54.
3. Courchesne E. Brain development in autism: early overgrowth followed by premature arrest of growth. *Ment Retard Dev Disabil Res Rev*. 2004;10(2):106–11.
4. Courchesne E, Campbell K, Solso S. Brain growth across the life span in autism: age-specific changes in anatomical pathology. *Brain Res*. 2011;1380:138–45.
5. Schumann CM, Bloss CS, Barnes CC, et al. Longitudinal magnetic resonance imaging study of cortical development through early childhood in autism. *J Neurosci*. 2010;30(12):4419–27.
6. Courchesne E, Mouton PR, Calhoun ME, et al. Neuron number and size in prefrontal cortex of children with autism. *JAMA*. 2011;306(18):2001–10
7. Stoner R, Chow ML, Boyle MP, et al. Patches of disorganization in the neocortex of children with autism. *N Engl J Med*. 2014;370(13):1209–19.
8. Régis J, Mangin J-F, Ochiai T, et al. "Sulcal root" generic model: a hypothesis to overcome the variability of the human cortex folding patterns. *Neurol Med Chir*. 2005;45(1):1–17.
9. Armstrong E, Schleicher A, Omran H, Curtis M, Zilles K. The Ontogeny of Human Gyrification. *Cereb Cortex* . 1995;5 (1):56–63.
10. Van Essen DC. A tension-based theory of morphogenesis and compact wiring in the central nervous system. *Nature*. 1997;385:313–8.
11. Zilles K, Palomero-Gallagher N, Amunts K. Development of cortical folding during evolution and ontogeny. *Trends Neurosci*. 2013;36(5):275–84.
12. Chenn A, Walsh C. Regulation of cerebral cortical size by control of cell cycle exit in neural precursors. *Science.* 2002;297:365–9.

13. Williams EL, El-Baz A, Nitzken M, Switala AE, Casanova MF. Spherical harmonic analysis of cortical complexity in autism and dyslexia. *Transl Neurosci*. 2012;3(1):36–40.

14. Nordahl CW, Dierker D, Mostafavi I, et al. Cortical folding abnormalities in autism revealed by surface-based morphometry. *J Neurosci*. 2007;27(43):11725–35.

15. Auzias G, Viellard M, Takerkart S, et al. Atypical sulcal anatomy in young children with autism spectrum disorder. *NeuroImage Clin*. 2014;4:593–603.

16. Levitt JG, Blanton RE, Smalley S, et al. Cortical sulcal maps in autism. *Cereb Cortex*. 2003;13(7):728–35.

17. Wallace GL, Robustelli B, Dankner N, Kenworthy L, Giedd JN, Martin A. Increased gyrification, but comparable surface area in adolescents with autism spectrum disorders. *Brain*. 2013;136:1956–67.

18. Schaer M, Ottet M-C, Scariati E, et al. Decreased frontal gyrification correlates with altered connectivity in children with autism. *Front Hum Neurosci*. 2013;7:750.

19. Nie J, Guo L, Li K, et al. Axonal fiber terminations concentrate on gyri. *Cereb Cortex*. 2012;22(12):2831–9.

20. Vandekar SN, Shinohara RT, Raznahan A, et al. Topologically dissociable patterns of development of the human cerebral cortex. *J Neurosci*. 2015;35(2):599–609.

21. Hoppenbrouwers M, Vandermosten M, Boets B. Autism as a disconnection syndrome: A qualitative and quantitative review of diffusion tensor imaging studies. *Res Autism Spectr Disord*. 2014;8(4):387–412.

22. Travers BG, Adluru N, Ennis C, et al. Diffusion tensor imaging in autism spectrum disorder: a review. *Autism Res*. 2012;5(5):289–313.

23. Di Martino A, Yan C-G, Li Q, et al. The autism brain imaging data exchange: towards a large-scale evaluation of the intrinsic brain architecture in autism. *Mol Psychiatry*. 2014; 19:659–67.

24. Parellada M, Boada L, Moreno C, et al. Specialty Care Programme for autism spectrum disorders in an urban population: A case-management model for health care delivery in an ASD population. *Eur Psychiatry*. 2013;28(2):102–9.

25. Parellada M, Moreno C, Mac-Dowell K, et al. Plasma antioxidant capacity is reduced in Asperger syndrome. *J Psychiatr Res*. 2012;46(3):394–401.

26. American Psychiatric Association. *Diagnostic and Statistical Manual of Mental Disorders*. 4th ed. Washington DC: American Psychiatric Publishing; 1994.

27. Gillberg IC, Gillberg C. Asperger syndrome—some epidemiological considerations: a research note. *J Child Psychol Psychiatry*. 1989;30(4):631–638.

28. Hollingshead AB, Redlich FC. *Social Class and Mental Illness*. New York: Wiley; 1958.

29. Ezpeleta L, Granero R, de la Osa N. Evaluación del deterioro en niños y adolescentes a través de la Children's Global Assessment Scale (CGAS). *Rev Psiquiatr Infanto-Juvenil*. 1999;1:18–26.

30. Shaffer D, Gould MS, Brasic J, Ambrosini P, Fisher P, Bird H. A children's global assessment scale (CGAS). *Arch Gen Psychiatry*. 1983;40(11):1228–1231.

31. Wechsler D. Wechsler intelligence scale for children, revised: WISC-R; manual. *Psychol Corp*. 1974.

32. Wechsler D. WAIS-III: Wechsler Adult Intelligence Scale (3rd ed.). *Psychol Corp Brace, San Antonio, TX*. 1997.

33. Merchán-Naranjo J, Mayoral M, Rapado-Castro M, et al. Estimation of the intelligence quotient using Wechsler Intelligence Scales in children and adolescents with Asperger syndrome. *J Autism Dev Disord*. 2012;42(1):116–22.

34. Dennis M, Francis DJ, Cirino PT, Schachar R, Barnes MA, Fletcher JM. Why IQ is not a covariate in cognitive studies of neurodevelopmental disorders. *J Int Neuropsychol Soc*. 2009;15(3):331–43.

35. Buchanan RW, Heinrichs DW. The Neurological Evaluation Scale (NES): a structured instrument for the assessment of neurological signs in schizophrenia. *Psychiatry Res*. 1989;27(3):335–50.

36. Dale AM, Fischl B, Sereno MI. Cortical Surface-Based Analysis: I. Segmentation and Surface Reconstruction. 1999;9:179–194.

37. Desikan RS, Ségonne F, Fischl B, et al. An automated labeling system for subdividing the human cerebral cortex on MRI scans into gyral based regions of interest. *Neuroimage*. 2006;31(3):968–80.

38. Fischl B, Sereno MI, Dale AM. Cortical Surface-Based Analysis: II. Inflation, Flattening, and a Surface-Based Coordinate System Bruce. 1999;9:195–207.

39. Su S, White T, Schmidt M, Kao C-Y, Sapiro G. Geometric computation of human gyrification indexes from magnetic resonance images. *Hum Brain Mapp*. 2013;34(5):1230–44.

40. Zilles K, Armstrong E, Schleicher A, Kretschmann H. Anatomy and Embryology The human pattern of gyrification in the cerebral cortex. *Anat Embryol*. 1988;179:173–179.

41. Jou RJ, Mateljevic N, Kaiser MD, Sugrue DR, Volkmar FR, Pelphrey KA. Structural neural phenotype of autism: preliminary evidence from a diffusion tensor imaging study using tract-based spatial statistics. *Am J Neuroradiol*. 2011;32(9):1607–13.

42. Thomas C, Humphreys K, Jung K-J, Minshew N, Behrmann M. The anatomy of the callosal and visual-association pathways in high-functioning autism: a DTI tractography study. *Cortex*. 2010;47(7):863–73.

43. Yendiki A, Panneck P, Srinivasan P, et al. Automated probabilistic reconstruction of white-matter pathways in health and disease using an atlas of the underlying anatomy. *Front Neuroinform*. 2011;5:23.

44. Smith SM, Jenkinson M, Johansen-Berg H, et al. Tract-based spatial statistics: voxelwise analysis of multi-subject diffusion data. *Neuroimage*. 2006;31(4):1487–505.

45. Smith SM, Jenkinson M, Woolrich MW, et al. Advances in functional and structural MR image analysis and implementation as FSL. *Neuroimage*. 2004;23 Suppl 1:S208–19.

46. Nichols TE, Holmes AP. Nonparametric permutation tests for functional neuroimaging: a primer with examples. *Hum Brain Mapp*. 2002;15(1):1–25.

47. Li G, Wang L, Shi F, et al. Mapping longitudinal development of local cortical gyrification in infants from birth to 2 years of age. *J Neurosci*. 2014;34(12):4228–38.

48. Raznahan A, Shaw P, Lalonde F, et al. How does your cortex grow? *J Neurosci*. 2011;31(19):7174–7.

49. Klein D, Rotarska-Jagiela A, Genc E, et al. Adolescent brain maturation and cortical folding: evidence for reductions in gyrification. *PLoS One*. 2014;9: e84914.

50. White T, Su S, Schmidt M, Kao C-Y, Sapiro G. The development of gyrification in childhood and adolescence. *Brain Cogn*. 2010;72(1):36–45.

51. Libero LE, DeRamus TP, Deshpande HD, Kana RK. Surface-based morphometry of the cortical architecture of autism spectrum Disorders: Volume, thickness, area, and gyrification. *Neuropsychologia*. 2014;62:1–10.

52. Toro R, Perron M, Pike B, et al. Brain size and folding of the human cerebral cortex. *Cereb Cortex*. 2008;18(10):2352–7.

53. Ecker C, Ronan L, Feng Y, et al. Intrinsic gray-matter connectivity of the brain in adults with autism spectrum disorder. *Proc Natl Acad Sci*. 2013;110(32):13222–7.

54. Dennis EL, Jahanshad N, McMahon KL, et al. Development of brain structural connectivity between ages 12 and 30: a 4-Tesla diffusion imaging study in 439 adolescents and adults. *Neuroimage*. 2013;64:671–84.

55. Hagmann P, Sporns O, Madan N, et al. White matter maturation reshapes structural connectivity in the late developing human brain. *Proc Natl Acad Sci*. 2010;107(44):19067–72.

56. Lebel C, Gee M, Camicioli R, Wieler M, Martin W, Beaulieu C. Diffusion tensor imaging of white matter tract evolution over the lifespan. *Neuroimage*. 2012;60(1):340–52.

57. Lee JE, Bigler ED, Alexander AL, et al. Diffusion tensor imaging of white matter in the superior temporal gyrus and temporal stem in autism. *Neurosci Lett*. 2007;424(2):127–32.

58. Cheng Y, Chou K-H, Chen I-Y, Fan Y-T, Decety J, Lin C-P. Atypical development of white matter microstructure in adolescents with autism spectrum disorders. *Neuroimage*. 2010;50(3):873–82.

59. Shukla DK, Keehn B, Lincoln AJ, Müller R-A. White matter compromise of callosal and subcortical fiber tracts in children with autism spectrum disorder: a diffusion tensor imaging study. *J Am Acad Child Adolesc Psychiatry*. 2010;49(12):1269–78.

60. Paul LK, Corsello C, Kennedy DP, Adolphs R. Agenesis of the corpus callosum and autism: a comprehensive comparison. *Brain*. 2014;137(6):1813–1829.

61. Casanova MF, El-Baz A, Mott M, et al. Reduced gyral window and corpus callosum size in autism: possible macroscopic correlates of a minicolumnopathy. *J Autism Dev Disord*. 2009;39(5):751–64.

62. Belmonte MK, Allen G, Beckel-Mitchener A, Boulanger LM, Carper RA, Webb SJ. Autism and abnormal development of brain connectivity. *J Neurosci*. 2004;24(42):9228–31.

63. Song S-K, Yoshino J, Le TQ, et al. Demyelination increases radial diffusivity in corpus callosum of mouse brain. *Neuroimage*. 2005;26(1):132–40.

Table 1. Demographic and Clinical Characteristics of the Madrid Sample

	ASD (n = 30)	**TDC (n = 29)**	*P*
Age (yrs) mean (SD) [range]	12.7 (2.5) [8-18]	12.5 (2.8) [7-18]	.79
Sex (males/females)	29/1	28/1	.98
Hand preference (right/left/ambidextrous)[a]	26/1/2	23/1/3	.86

Total IQ[b] mean (SD) [range]	91.8 (20.1) [53-134]	112.0 (13.4) [70-138]	<.001***
Verbal IQ mean (SD) [range]	93.7 (25.1) [51-139]	-	
Vocabulary	9.1 (4.3)	11.2 (2.9)	.02
Performance IQ[b] mean (SD) [range]	87.1 (22.0) [44-132]	-	
Block Design	8.2 (3.2)	11.5 (2.5)	<.001***
Parental education (yrs)	14.2 (3.2)	14.0 (3.2)	.62
Participant Education (yrs)	6.8 (2.8)	7.8 (2.5)	.19
Socioeconomic status	3.5 (1.3)	3.8 (1.2)	.46
Clinical characterization			
CGAS	49.2 (12.7)	94.2 (4.1)	<.001***
Gillberg total score	12.6 (3.1)	-	
Medication - n (%)			
None	22 (73%)		
APS	8 (27%)		

Note: APS = Antipsychotic medication; ASD = autism spectrum disorders; CGAS = Children's Global Assessment Scale; SD = standard deviation; TDC = typically developing children.

[a] Information on hand preference was missing for 3 participants

[b] Total IQ was estimated for typically developing participants. Verbal and performance IQ were not available for typically developing children; vocabulary and block design subtest scores are reported for purposes of comparison.

Table 2. Demographic and Clinical Characteristics of the ABIDE Replication Sample.

	ASD **(n = 39)**	**TDC** **(n = 65)**	*P*
Age (yrs) mean (SD) [range]	12.0 (2.6) [9-18]	12.8 (2.8) [8-18]	.20
Sex (males/females)	34/5	48/17	.14
Total IQ mean (SD) [range]	107 (15.8) [78-148]	111 (14) [80-138]	.11
Verbal IQ mean (SD) [range]	105 (15.4) [77-139]	112 (13.3) [80-143]	.01**
Performance IQ mean (SD) [range]	108 (16.3) [79-147]	109 (15) [67-137]	.93
Clinical characterization			
ADI-R Social	18.9 (5.2) [7-27]		
ADI-R Verbal	15.21 (4.2) [8-23]		
ADI-R RRB	5.9 (2.9) [0-12]		
ADI-R Onset	3.2 (1.2) [1-5]		
ADOS Total	10.9 (3.9) [5-22]		
ADOS Communication	3.4 (1.5) [1-8]		
ADOS Social	7.5 (2.8) [2-14]		
ADOS Stereotype Behavior	2.3 (1.3) [0-5]		
Medication - n (%)			
None	32 (82%)		
APS	-		
Non-APS	7 (18%)		

Note: ADI-R = Autism Diagnostic Interview – Revised; ADOS = Autism Diagnostic Observation Schedule; APS = Antipsychotic medication; ASD = autism spectrum disorders; RRB = repetitive and ritualistic behavior; SD = standard deviation; TDC = typically developing children.

Figure 1: Age-related differences in left prefrontal (left) and parietal (right) gyrification index (GI) between participants with autism spectrum disorders (ASD) and typically developing controls (analysis of covariance [ANCOVA] with age as covariate). Note: A similar pattern was found in the replication sample from the Autism Brain Imaging Data Exchange (ABIDE) initiative (lower row).

Figure 2: Age-related differences in fractional anisotropy (FA) and radial diffusivity (RD) in the forceps minor (left column) between participants with autism spectrum disorders (ASD) and typically developing controls. Note: These findings were confirmed by hypothesis-free voxel-wise tract-based spatial statistics showing local age-related group differences in the forceps minor (right column, after correction for multiple comparisons). For the largest FA and RD cluster, participants' values were averaged over the voxels belonging to the cluster, multiplied by 100, and plotted against age. AD = axial diffusivity.

Figure 3: The relationship between tractography-based fractional anisotropy (FA) and radial diffusivity (RD) measures of the forceps minor and left prefrontal gyrification index. Note: Participants with autism spectrum disorders (ASD) show a different relationship between forceps minor RD (right column), but not FA (left column), and the left prefrontal gyrification index compared to typically developing controls. Age was regressed out and the measurements were plotted as unstandardized residuals. The prefrontal gyrification index is defined as the ratio of the prefrontal pial surface area (yellow line) and the prefrontal hull surface area (red line).

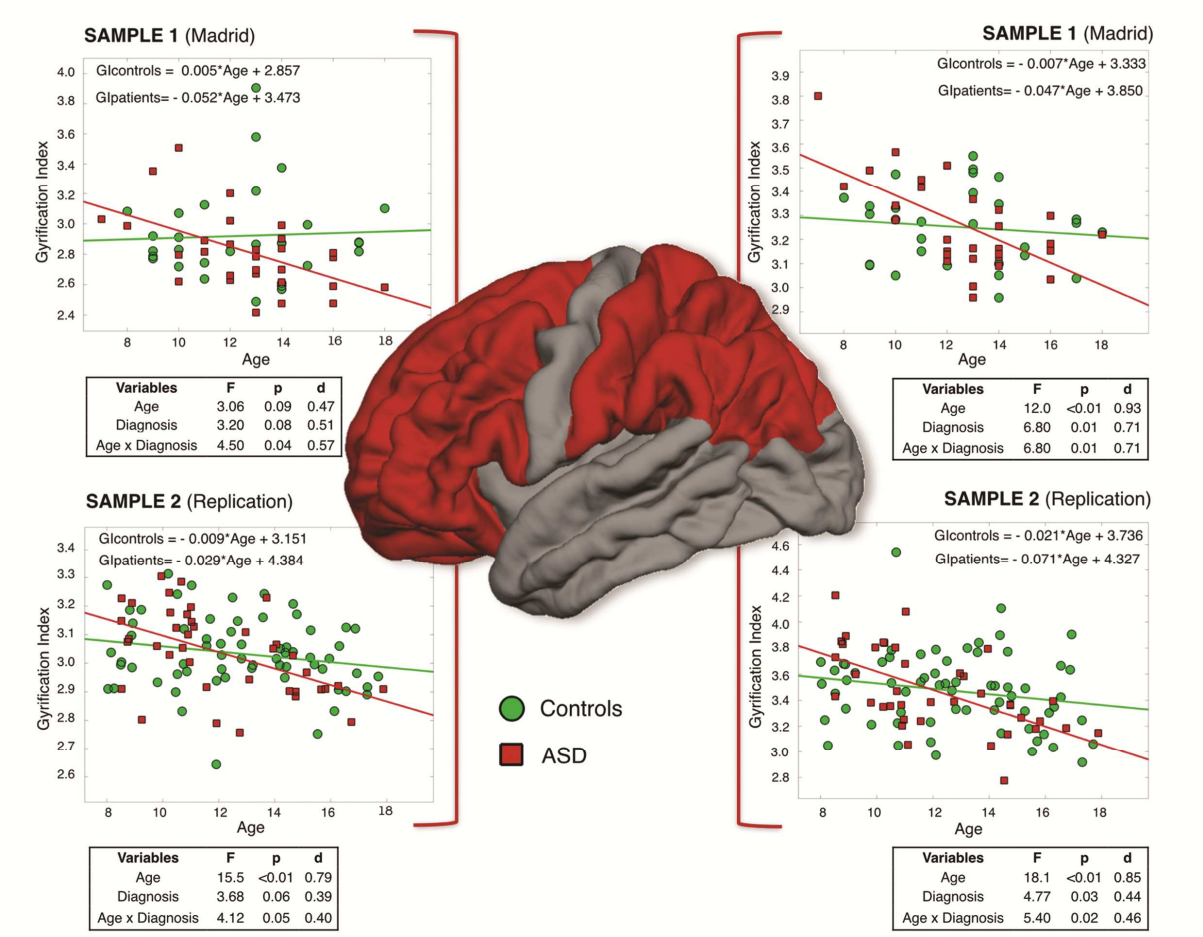

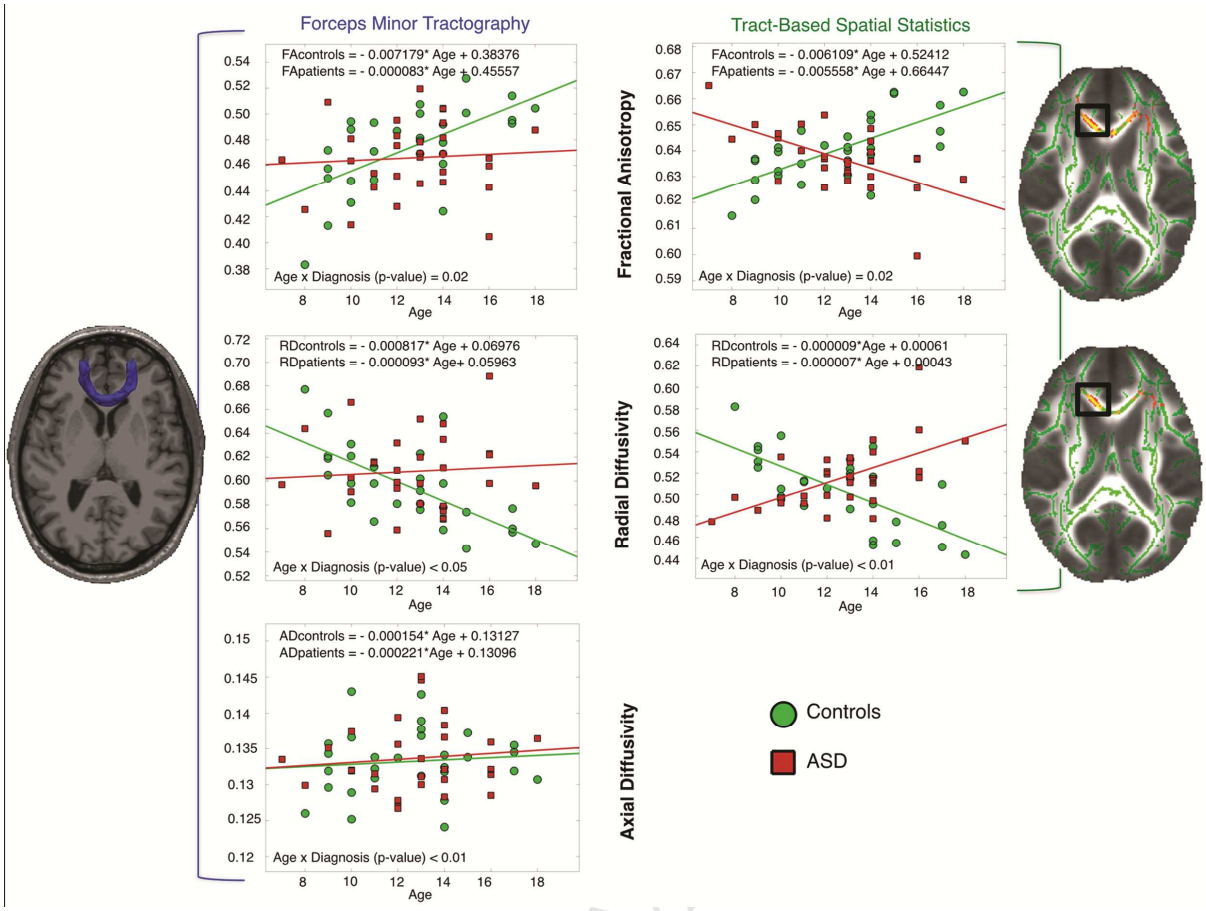

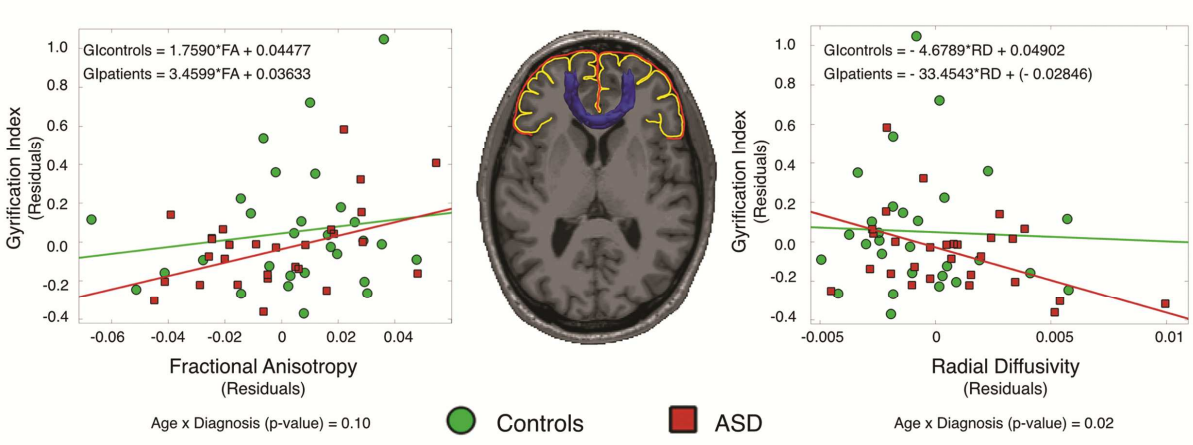

Supplement 1

Madrid Sample: Diagnostic Assessment

Board-certified child and adolescent psychiatrists with extensive experience in the field of autism spectrum disorders (ASD) conducted all diagnostic assessments. They conducted a developmental, medical, and psychiatric interview with the parents and a child observation. They administered the Spanish-language version of the Schedule for Affective Disorders and Schizophrenia for School-Age Children–Present and Lifetime Version (K-SADS-PL)[1] to rule out comorbid psychiatric disorders. In any doubtful case, a consensus agreement was sought with another of the evaluating child psychiatrists. If consensus was not reached, the ADOS-G (Autism Diagnostic Observation Schedule–Generic)[2] was administered by experienced ADOS research-trained child psychiatrists (9 instances), one of them an ADOS trainer herself (M.P.). The final diagnosis was based on best clinical judgment taking into account all the available information.[2,3]

The K-SADS was also administered to typically developing controls in order to rule out any psychiatric condition. It was administered individually to parents and children in separate interviews by trained and experienced psychiatrists.

Replication Sample: Inclusion of the New York University (NYU) Langone Medical Center Sample

The NYU Langone Medical Center sample is part of the Autism Brain Imaging Data Exchange (ABIDE[4]) repository (http://fcon_1000.projects.nitrc.org/indi/abide/). ABIDE is a grass-roots initiative providing previously collected magnetic resonance imaging (MRI) datasets and phenotypic information from individuals with ASD and age-matched typically developing controls to promote data sharing and discovery science in the broader scientific community. We selected this site within the ABIDE repository because it provided well-distributed data along the developmental continuum from late childhood to early adulthood.

All participants from the NYU Langone sample within the same age range as the Madrid sample were initially included in the replication dataset. Detailed information on

recruitment procedures, inclusion and exclusion criteria, and clinical and cognitive assessments for these participants is provided on the ABIDE website.[4] Before starting, participants and their parents or legal guardians signed an informed consent document after receiving an explanation of the study procedures.

Replication Sample: MRI Acquisition and Participant Exclusion

All participants were scanned on the same 3T Siemens Allegra scanner. A T1-weighted 3D volumetric image with a voxel size of 1.3x1.3x1.0 mm^3 (TR = 2530 ms, TE = 3.25 ms, flip angle = 7º) was acquired. As stated on the ABIDE website, the ABIDE dataset is distributed without any quality control; therefore, intensive empirical inspection was performed for each participant. This led to the exclusion of 29 participants, listed in Table S3 along with the reason for their exclusion. In total, 39 children with ASD and 65 typically developing children were included in the replication sample that was used for analysis.

Replication Sample: Comparison of Excluded Participants and Remaining Participants

We compared the excluded participants with the remaining participants and found no differences in demographic or cognitive measures (Table S4). From the remaining sample (n=156), we selected all participants within the same age-range as the Madrid sample, resulting in a final sample of 104 participants (39 participants with ASD, 65 typically developing controls).

Madrid Sample: MRI Acquisition Parameters

Three MRI scans were acquired sequentially: A T1-weighted 3D volumetric image consisting of 175 contiguous sagittal slices, with a voxel size of 1x0.94x0.94 mm^3 (repetition time (TR) = 25 ms, echo time (TE) = 9.2 ms, flip angle = 30º), a T2-weighted turbo spin echo scan, voxels size 1x1x3 mm^3 (TR = 5809 ms, TE = 120 ms), and a diffusion tensor image (DTI) scan consisting of 60 axial slices with 15 directions, with a voxel size of 1.75x1.75x2 mm^3 (b0 = 800 ms, TR = 10927 ms, TE = 82 ms, flip angle = 90º). Both T1-

and T2-weighted images were used for clinical neurodiagnostic evaluation by an independent neuroradiologist. No participants showed clinically significant brain pathology.

Madrid and Replication Sample: Surface Area and Gyrification Index

Following the method by Su and colleagues,[5] a 3D brain envelope was computed per lobe as follows: first, the cortical gyral parcellation of FreeSurfer's 'aparc+aseg' volumetric image was relabeled prefrontal, parietal, temporal and occipital, in accordance with the surface-based lobar parcellation. Second, the brain envelope was defined per hemisphere as the area of a smooth envelope that wrapped around the hemisphere but did not encroach into the sulci. In order to generate the envelope, a morphological isotropic closing of 6 mm was applied to the relabeled 'aparc+aseg' image to ensure smooth boundaries. Then, an unlabeled envelope was created using the marching cubes algorithm. Finally, the envelope was parcellated into lobes using the smoothed parcellated volumetric image and a nearest neighbor interpolation algorithm (Figure S1). This parcellation includes the insula but not the cingulate cortex, as this structure cannot be assigned to a single lobe. This also permitted quantification of the surface area (SA) of the brain envelope.[6,7] The Matlab scripts used for generating the parcellated brain envelope can be found at: ftp://disco.hggm.es/jjanssen/adoles_surfgmdevelop/scripts/.

Madrid-Sample: DTI Preprocessing and Data Quality Assessment

In order to detect and correct any artifacts introduced during collection of the DTI scan, a quality control protocol was implemented. First, artifacts related to intensity were detected by computing the normalized correlation between intensity in successive slices across the diffusion volume. Any diffusion volumes containing one or more artifacts were excluded. Next, eddy-current and head motion correction was performed using FSL (www.fmrib.ox.ac.uk/fsl/) tools.[8] Finally, machine-related (i.e., B0 field inhomogeneity) spatial distortions were corrected by warping each participant's T2-b0 image to the anatomical T2-weighted image of the same individual. This technique produces (a) a warp-

field, which was applied to the participant's diffusion volumes and (b) a Jacobian map of the warp-field, which was multiplied with the participant's warped diffusion volumes in order to restore true image intensity after warping. To achieve high dimensional and robust warping, we computed large-deformation diffeomorphic mapping using the symmetric normalization (SyN) technique implemented in the Advance Normalization Tools (ANTS) software package (http://stnava.github.io/ANTs/).[9] This warp-field was applied to the anterior-posterior axis of the participant, i.e. the phase-encoding direction (y-coordinate), reducing the geometric distortion that was present along that axis, while preserving the signal in the other axes.

Data quality was quantified using four different measures (average translation, average rotation, percentage bad slices, and average drop-out score). These four motion measures capture global frame-to-frame motion as well as the frequency and severity of rapid slice-to-slice motion.[10] We compared these measures between groups and found only minor differences that did not reach statistical significance (Table S5).

References

1. Kaufman J, Birmaher B, Brent D, et al. Schedule for Affective Disorders and Schizophrenia for School-Age Children-Present and Lifetime Version (K-SADS-PL): initial reliability and validity data. *J Am Acad Child Adolesc Psychiatry*. 1997;36:980-988.

2. Lord C, Petkova E, Hus V, et al. A multisite study of the clinical diagnosis of different autism spectrum disorders. *Arch Gen Psychiatry*. 2012;69(3):306-313.

3. Volkmar F, Siegel M, Woodbury-Smith M, King B, McCracken J, State M. Practice parameter for the assessment and treatment of children and adolescents with autism spectrum disorder. *J Am Acad Child Adolesc Psychiatry*. 2014;53(2):237-257.

4. Di Martino A, Yan C-G, Li Q, et al. The autism brain imaging data exchange: towards a large-scale evaluation of the intrinsic brain architecture in autism. *Mol Psychiatry*. 2013:1-9.

5. Su S, White T, Schmidt M, Kao C-Y, Sapiro G. Geometric computation of human gyrification indexes from magnetic resonance images. *Hum Brain Mapp*. 2013;34(5):1230-1244.

6. Alemán-Gómez Y, Janssen J, Schnack H, et al. The human cerebral cortex flattens during adolescence. *J Neurosci*. 2013;33(38):15004-15010.

7. Janssen J, Alemán-Gómez Y, Schnack H, et al. Cortical morphology of adolescents with bipolar disorder and with schizophrenia. *Schizophr Res*. 2014;158(1-3):91-99.

8. Smith SM, Jenkinson M, Woolrich MW, et al. Advances in functional and structural MR image analysis and implementation as FSL. *Neuroimage*. 2004;23 Suppl 1:S208-S219.

9. Avants BB, Tustison NJ, Song G, Cook P a, Klein A, Gee JC. A reproducible evaluation of ANTs similarity metric performance in brain image registration. *Neuroimage*. 2011;54(3):2033-2044.

10. Yendiki A, Koldewyn K, Kakunoori S, Kanwisher N, Fischl B. Spurious group differences due to head motion in a diffusion MRI study. *Neuroimage*. 2013;88C:79-90.

Table S1. Whole-Brain Characteristics of the Madrid Sample

	ASD (n = 30)	TDC (n = 29)	*P*
Whole-brain characteristics[a]			
Cortical volume (cm^3)	528.5 (58.9) [414.7-642.4]	534.6 (45.8) [441.7-639.1]	0.54
Cortical surface area (cm^2)	2111.4 (214.6) [1636.0-2475.5]	2175.2 (179.3) [1854.1-2565.4]	0.70
Whole brain GI	2.7 (0.2) [2.4-3.1]	2.8 (0.1) [2.6-3.1]	0.21
Prefrontal GI	2.9 (0.3) [2.4-3.7]	3.0 (0.3) [2.5-3.9]	0.11
Parietal GI	3.3 (0.2) [2.9-3.6]	3.3 (0.1) [3.1-3.5]	0.68
Temporal GI	2.7 (0.3) [2.3-3.5]	2.8 (0.3) [2.3-3.6]	0.31
Occipital GI	2.1 (0.2) [1.9-2.5]	2.1 (0.1) [1.7-2.4]	0.51

Note: ASD = autism spectrum disorder; GI = gyrification index; TDC = typically developing children.

[a]Differences in whole-brain characteristics within the Madrid sample tested with Student's t-tests.

Table S2. Whole-Brain Characteristics of the Autism Brain Imaging Data Exchange (ABIDE) Replication Sample

	ASD (n = 39)	TDC (n = 65)	*P*
Whole-brain characteristics[a]			
Cortical volume (cm^3)	565.3 (64.3) [433.4-712.9]	564 (54.6) [431.9-677.5]	0.91
Cortical surface area (cm^2)	2156.3 (224.7) [1651.7-2659.1]	2175.2.9 (179.3) [1854.1-2565.4]	0.64
Whole-brain GI	2.8 (0.1) [2.6-3.0]	2.8 (0.1) [2.4-3.0]	0.99
Prefrontal GI	3.0 (0.1) [2.7-3.2]	3.0 (0.1) [2.6-3.2]	0.86
Parietal GI	3.6 (0.3) [3.1-4.1]	3.6 (0.3) [3.0-4.5]	0.98
Temporal GI	2.7 (0.2) [2.2-2.9]	2.6 (0.2) [2.0-3.1]	0.79
Occipital GI	1.8 (0.1) [1.6-2.0]	1.8 (0.1) [1.7-2.0]	0.68

Note: ASD = autism spectrum disorder; GI = gyrification index; TDC = typically developing children.

[a]Differences in whole-brain characteristics within the replication sample tested with Student's t-tests.

Table S3. Excluded Participants From the Autism Brain Imaging Data Exchange (ABIDE) Sample

ABIDE Code	Reason for Exclusion
0050967	severe loss of signal in posterior part of the brain
0050978	movement artifact in occipital part of the brain
0050979	artifact in anterior frontal part of the brain
0050982	artifact in the occipital part of the brain
0050984	severe loss of signal in posterior part of the brain
0050987	diffuse movement artifact
0050988	severe loss of signal in posterior part of the brain
0050989	artifact in inferior part of the brain
0050998	diffuse movement artifact
0051000	movement artifact in occipital lobe
0051003	diffuse movement artifact
0051016	foldover artifact
0051024	incomplete image acquisition
0051030	artifact in occipital lobe
0051033	diffuse movement artifact
0051034	artifact in occipital lobe
0051064	movement artifact in occipital lobe
0051070	diffuse artifact in medial part of the brain
0051079	severe loss of signal in posterior part of the brain
0051088	severe loss of signal in posterior part of the brain
0051091	diffuse movement artifact
0051099	artifact in posterior part of the brain
0050953	asymetric lateral ventricles
0050955	incomplete image acquisition
0050960	severe loss of signal in posterior part of the brain
0050961	artifact in occipital part of the brain
0051042	incomplete image acquisition
0051050	severe loss of signal in posterior part of the brain

Table S4. Comparison of the Excluded (Based on the Quality of the T1-Weighted Scan) and Remaining Participants of the Replication Sample.

	Remaining Participants (n = 156)	**Excluded (n = 29)**	*P*
Age (yrs) mean (SD) [range]	15.5 (15.6) [7-32]	13.5 (8.3) [7-39]	0.12
Sex (males/females)	125/31	22/6	0.8
Hand preference (left/right)	13/138	5/23	0.15
Estimated IQ	111 (14.1) [78-148]	111 (19) [76-142]	0.89
Verbal IQ	110 (13.9) [73-143]	108 (18.2) [74-141]	0.49
Performance IQ	109 (14.7) [67-147]	111 (19.1) [72-149]	0.64

Note: SD = Standard Deviation.

Table S5. Between-Group Differences on the Four Measures of Diffusion Tensor Imaging Data Quality

	ASD (n = 30)	**TDC (n = 29)**	*P*
Average translation mean (SD)	0.9512 (0.3212)	1.0791 (0.4608)	0.22
Average rotation mean (SD)	0.0055 (0.0037)	0.0067 (0.0073)	0.43
Percentage bad slices mean (SD)	0	0.0790 (0.3878)	0.28
Average Dropout score mean (SD)	1	1.0065 (0.0307)	0.26

Note: ASD = autism spectrum disorder; SD = standard deviation; TDC = typically developing children.

Table S6. Demographic, Clinical, and Whole-Brain Characteristics of the Autism Brain Imaging Data Exchange (ABIDE) Replication Sample, Matched on Verbal IQ

	ASD (n = 39)	**TDC (n = 56)**	*P*
Age (yrs) mean (SD) [range]	12.0 (2.6) [9-18]	12.7 (3.0) [8-18]	0.26
Sex (males/females)	34/5	40/16	0.08
Estimated IQ	107 (15.8)	110 (13.8)	0.36
Verbal IQ	105 (15.4)	110 (12.9)	0.08
Performance IQ	108 (16.3)	107 (15.3)	0.77
Clinical characterization			
ADI-R Social	18.9 (5.2) [7-27]		
ADI-R Verbal	15.21 (4.2) [8-23]		
ADI-R RRB	5.9 (2.9) [0-12]		
ADI-R Onset	3.2 (1.2) [1-5]		
ADOS Total	10.9 (3.9) [5-22]		
ADOS Communication	3.4 (1.5) [1-8]		
ADOS Social	7.5 (2.8) [2-14]		
ADOS Stereotype Behavior	2.3 (1.3) [0-5]		
Medication - n (%)			
None	32 (82%)		
APS	-		
Non-APS	7 (18%)		
Whole-brain characteristics			
Cortical volume (cm^3)	565.3 (64.3) [433.4-712.9]	560 (52.3) [458-668.7]	0.69
Cortical surface area (cm^2)	2156.3 (224.7) [1651.7-2659.1]	2159.78 (170) [1855.1-2495.8]	0.95
Whole brain GI	2.8 (0.1) [2.6-3.0]	2.8 (0.1) [2.6-3.0]	0.98
Prefrontal GI	3.0 (0.1) [2.7-3.2]	3.0 (0.1) [2.7-3.2]	0.95
Parietal GI	3.6 (0.3) [3.1-4.1]	3.6 (0.3) [3.0-4.5]	0.88
Temporal GI	2.7 (0.2) [2.2-2.9]	2.7 (0.2) [2.3-3.1]	0.88
Occipital GI	1.8 (0.1) [1.6-2.0]	1.8 (0.1) [1.7-2.0]	0.77

Note: ADI-R = Autism Diagnostic Interview – Revised; ADOS = Autism Diagnostic Observation Schedule; APS = antipsychotic medication; ASD = autism spectrum disorder; GI = gyrification index; SD = standard deviation; TDC = typically developing children.

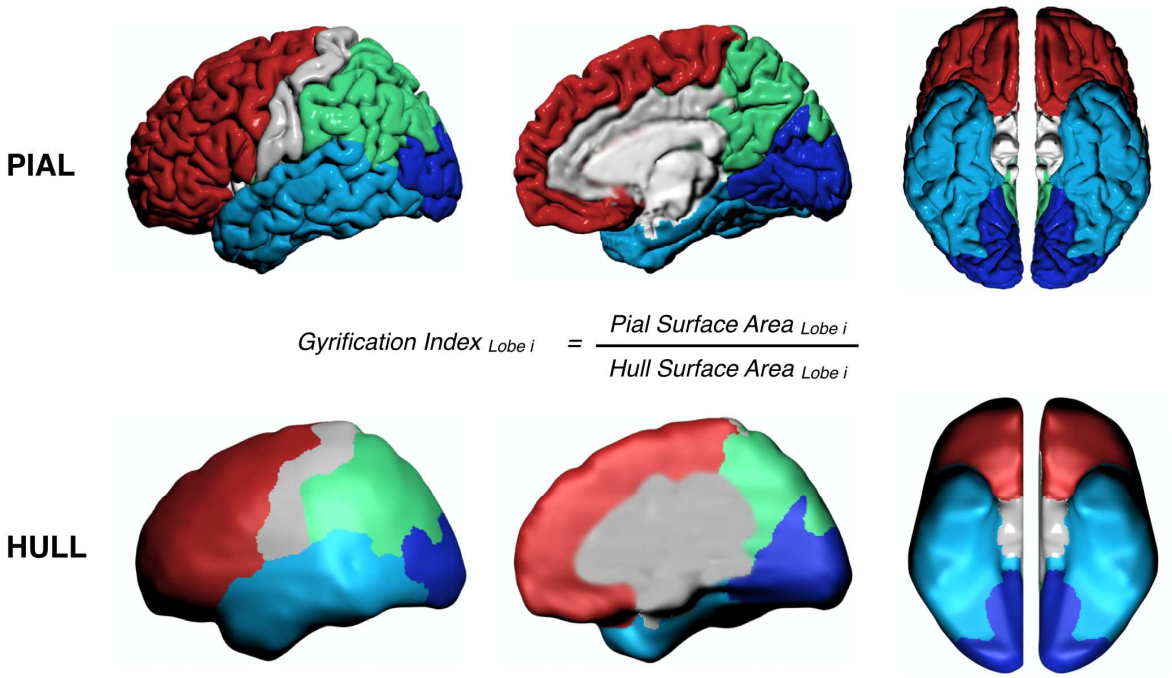

Supplementary Figure S1: 3D representations of the lateral, medial and ventral pial and hull segmentations

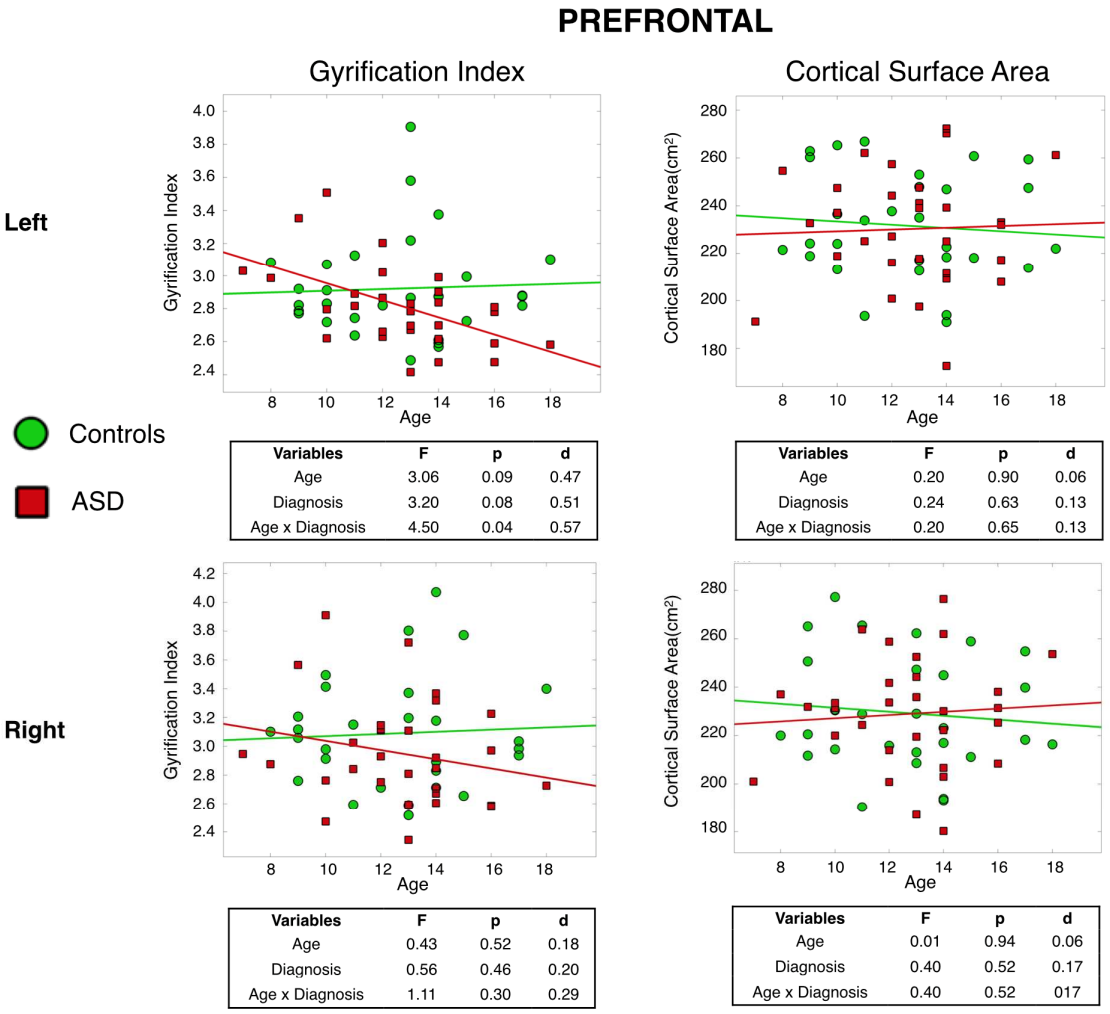

Variables	F	p	d
Age	3.06	0.09	0.47
Diagnosis	3.20	0.08	0.51
Age x Diagnosis	4.50	0.04	0.57

Variables	F	p	d
Age	0.20	0.90	0.06
Diagnosis	0.24	0.63	0.13
Age x Diagnosis	0.20	0.65	0.13

Variables	F	p	d
Age	0.43	0.52	0.18
Diagnosis	0.56	0.46	0.20
Age x Diagnosis	1.11	0.30	0.29

Variables	F	p	d
Age	0.01	0.94	0.06
Diagnosis	0.40	0.52	0.17
Age x Diagnosis	0.40	0.52	017

Supplementary Figure S2: Between-group differences in relative decrease in left prefrontal gyrification index. No differences were observed in right prefrontal gyrification index and bilateral prefrontal cortical surface area.

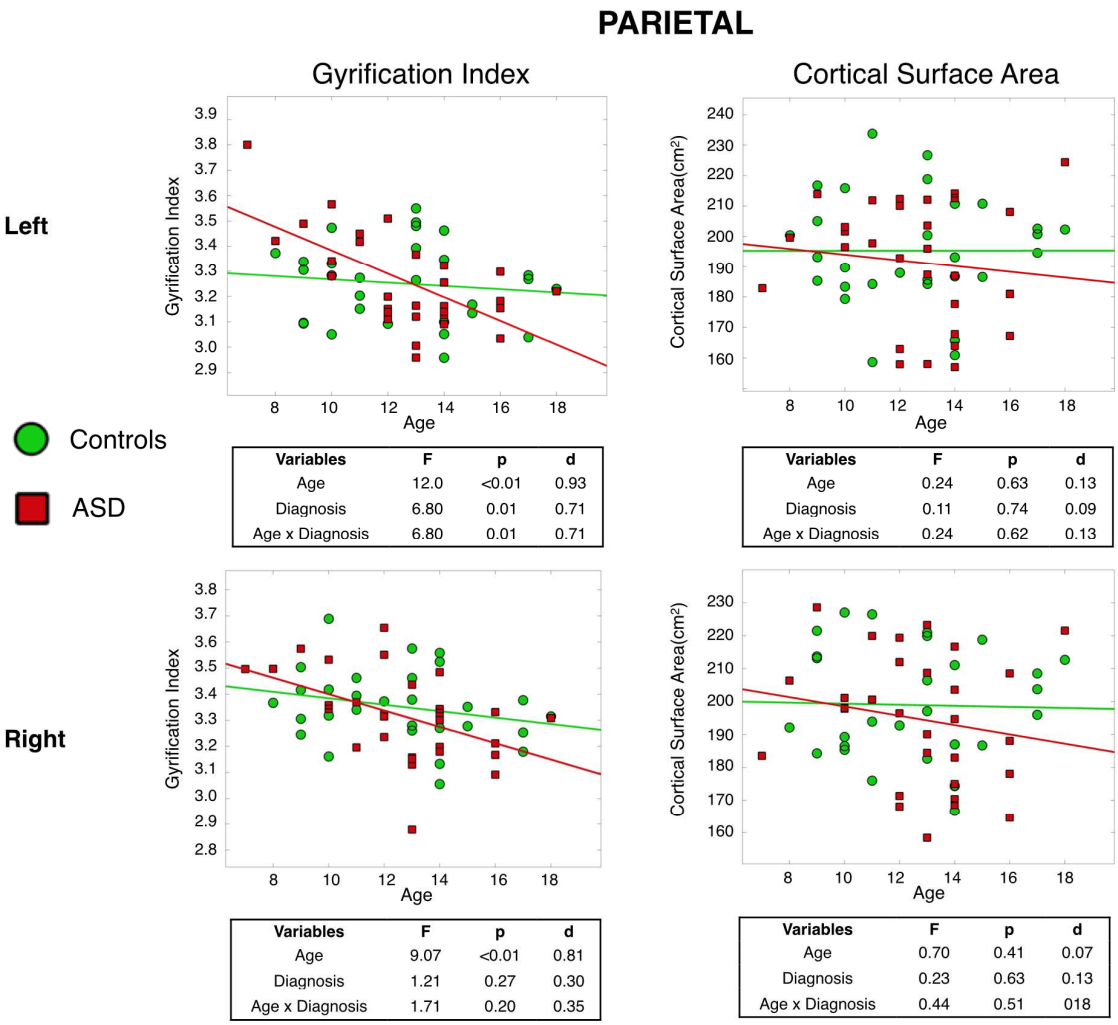

Supplementary Figure S3: Between-group differences in relative decrease in left parietal gyrification index. No differences were observed in right parietal gyrification index and bilateral parietal cortical surface area.

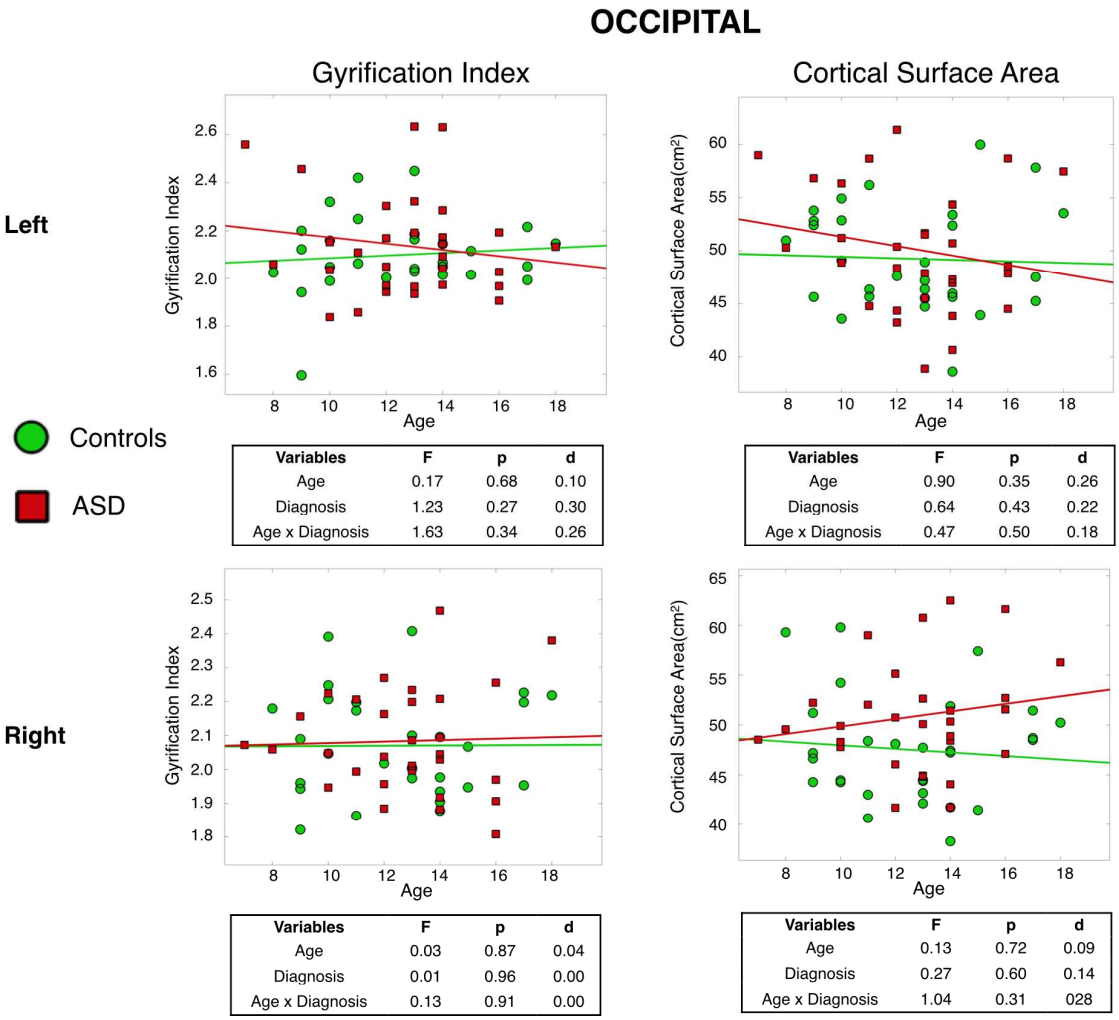

Supplementary Figure S4: No between-group differences in gyrification index and cortical surface area in the occipital lobes.

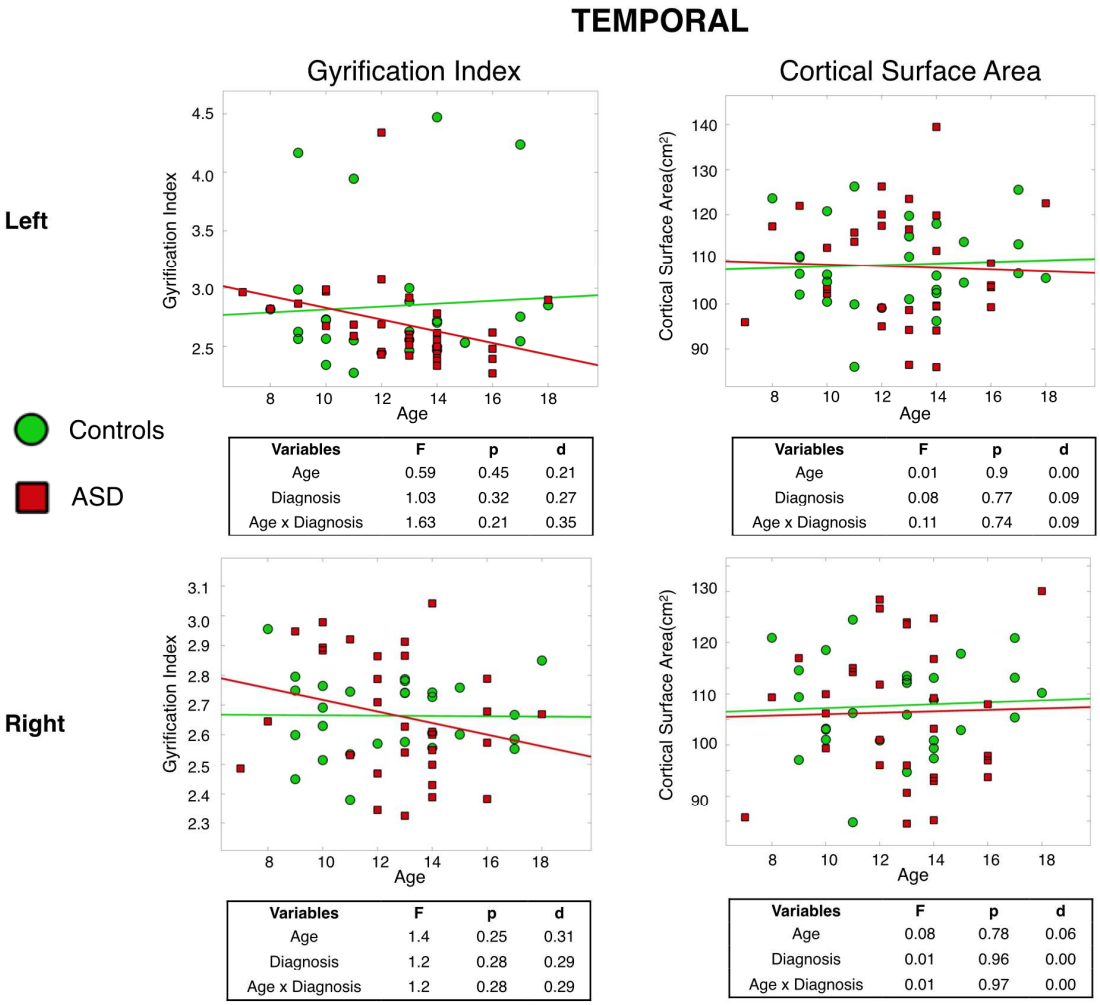

Supplementary Figure S5: No between-group differences in gyrification index and cortical surface area in the temporal lobes.